FERMILAB-PUB-08/451-E

Search for neutral Higgs bosons at high tanβ in the $b(h/H/A) \to b\tau^+\tau^-$ channel

V.M. Abazov[36], B. Abbott[75], M. Abolins[65], B.S. Acharya[29], M. Adams[51], T. Adams[49], E. Aguilo[6], M. Ahsan[59], G.D. Alexeev[36], G. Alkhazov[40], A. Alton[64,a], G. Alverson[63], G.A. Alves[2], M. Anastasoaie[35], L.S. Ancu[35], T. Andeen[53], B. Andrieu[17], M.S. Anzelc[53], M. Aoki[50], Y. Arnoud[14], M. Arov[60], M. Arthaud[18], A. Askew[49,b], B. Åsman[41], A.C.S. Assis Jesus[3], O. Atramentov[49], C. Avila[8], F. Badaud[13], L. Bagby[50], B. Baldin[50], D.V. Bandurin[59], P. Banerjee[29], S. Banerjee[29], E. Barberis[63], A.-F. Barfuss[15], P. Bargassa[80], P. Baringer[58], J. Barreto[2], J.F. Bartlett[50], U. Bassler[18], D. Bauer[43], S. Beale[6], A. Bean[58], M. Begalli[3], M. Begel[73], C. Belanger-Champagne[41], L. Bellantoni[50], A. Bellavance[50], J.A. Benitez[65], S.B. Beri[27], G. Bernardi[17], R. Bernhard[23], I. Bertram[42], M. Besançon[18], R. Beuselinck[43], V.A. Bezzubov[39], P.C. Bhat[50], V. Bhatnagar[27], G. Blazey[52], F. Blekman[43], S. Blessing[49], K. Bloom[67], A. Boehnlein[50], D. Boline[62], T.A. Bolton[59], E.E. Boos[38], G. Borissov[42], T. Bose[77], A. Brandt[78], R. Brock[65], G. Brooijmans[70], A. Bross[50], D. Brown[81], X.B. Bu[7], N.J. Buchanan[49], D. Buchholz[53], M. Buehler[81], V. Buescher[22], V. Bunichev[38], S. Burdin[42,c], T.H. Burnett[82], C.P. Buszello[43], P. Calfayan[25], S. Calvet[16], J. Cammin[71], M.A. Carrasco-Lizarraga[33], E. Carrera[49], W. Carvalho[3], B.C.K. Casey[50], H. Castilla-Valdez[33], S. Chakrabarti[72], D. Chakraborty[52], K.M. Chan[55], A. Chandra[48], E. Cheu[45], D.K. Cho[62], S. Choi[32], B. Choudhary[28], L. Christofek[77], T. Christoudias[43], S. Cihangir[50], D. Claes[67], J. Clutter[58], M. Cooke[50], W.E. Cooper[50], M. Corcoran[80], F. Couderc[18], M.-C. Cousinou[15], S. Crépé-Renaudin[14], V. Cuplov[59], D. Cutts[77], M. Ćwiok[30], H. da Motta[2], A. Das[45], G. Davies[43], K. De[78], S.J. de Jong[35], E. De La Cruz-Burelo[33], C. De Oliveira Martins[3], K. DeVaughan[67], F. Déliot[18], M. Demarteau[50], R. Demina[71], D. Denisov[50], S.P. Denisov[39], S. Desai[50], H.T. Diehl[50], M. Diesburg[50], A. Dominguez[67], T. Dorland[82], A. Dubey[28], L.V. Dudko[38], L. Duflot[16], S.R. Dugad[29], D. Duggan[49], A. Duperrin[15], S. Dutt[27], J. Dyer[65], A. Dyshkant[52], M. Eads[67], D. Edmunds[65], J. Ellison[48], V.D. Elvira[50], Y. Enari[77], S. Eno[61], P. Ermolov[38,‡], H. Evans[54], A. Evdokimov[73], V.N. Evdokimov[39], A.V. Ferapontov[59], T. Ferbel[61,71], F. Fiedler[24], F. Filthaut[35], W. Fisher[50], H.E. Fisk[50], M. Fortner[52], H. Fox[42], S. Fu[50], S. Fuess[50], T. Gadfort[70], C.F. Galea[35], C. Garcia[71], A. Garcia-Bellido[71], V. Gavrilov[37], P. Gay[13], W. Geist[19], W. Geng[15,65], C.E. Gerber[51], Y. Gershtein[49,b], D. Gillberg[6], G. Ginther[71], B. Gómez[8], A. Goussiou[82], P.D. Grannis[72], H. Greenlee[50], Z.D. Greenwood[60], E.M. Gregores[4], G. Grenier[20], Ph. Gris[13], J.-F. Grivaz[16], A. Grohsjean[25], S. Grünendahl[50], M.W. Grünewald[30], F. Guo[72], J. Guo[72], G. Gutierrez[50], P. Gutierrez[75], A. Haas[70], N.J. Hadley[61], P. Haefner[25], S. Hagopian[49], J. Haley[68], I. Hall[65], R.E. Hall[47], L. Han[7], K. Harder[44], A. Harel[71], J.M. Hauptman[57], J. Hays[43], T. Hebbeker[21], D. Hedin[52], J.G. Hegeman[34], A.P. Heinson[48], U. Heintz[62], C. Hensel[22,d], K. Herner[72], G. Hesketh[63], M.D. Hildreth[55], R. Hirosky[81], T. Hoang[49], J.D. Hobbs[72], B. Hoeneisen[12], M. Hohlfeld[22], S. Hossain[75], P. Houben[34], Y. Hu[72], Z. Hubacek[10], V. Hynek[9], I. Iashvili[69], R. Illingworth[50], A.S. Ito[50], S. Jabeen[62], M. Jaffré[16], S. Jain[75], K. Jakobs[23], C. Jarvis[61], R. Jesik[43], K. Johns[45], C. Johnson[70], M. Johnson[50], D. Johnston[67], A. Jonckheere[50], P. Jonsson[43], A. Juste[50], E. Kajfasz[15], D. Karmanov[38], P.A. Kasper[50], I. Katsanos[70], V. Kaushik[78], R. Kehoe[79], S. Kermiche[15], N. Khalatyan[50], A. Khanov[76], A. Kharchilava[69], Y.N. Kharzheev[36], D. Khatidze[70], T.J. Kim[31], M.H. Kirby[53], M. Kirsch[21], B. Klima[50], J.M. Kohli[27], J.-P. Konrath[23], A.V. Kozelov[39], J. Kraus[65], T. Kuhl[24], A. Kumar[69], A. Kupco[11], T. Kurča[20], V.A. Kuzmin[38], J. Kvita[9], F. Lacroix[13], D. Lam[55], S. Lammers[70], G. Landsberg[77], P. Lebrun[20], W.M. Lee[50], A. Leflat[38], J. Lellouch[17], J. Li[78,‡], L. Li[48], Q.Z. Li[50], S.M. Lietti[5], J.K. Lim[31], J.G.R. Lima[52], D. Lincoln[50], J. Linnemann[65], V.V. Lipaev[39], R. Lipton[50], Y. Liu[7], Z. Liu[6], A. Lobodenko[40], M. Lokajicek[11], P. Love[42], H.J. Lubatti[82], R. Luna-Garcia[33,e], A.L. Lyon[50], A.K.A. Maciel[2], D. Mackin[80], R.J. Madaras[46], P. Mättig[26], A. Magerkurth[64], P.K. Mal[82], H.B. Malbouisson[3], S. Malik[67], V.L. Malyshev[36], Y. Maravin[59], B. Martin[14], R. McCarthy[72], M.M. Meijer[35], A. Melnitchouk[66], L. Mendoza[8], P.G. Mercadante[5], M. Merkin[38], K.W. Merritt[50], A. Meyer[21], J. Meyer[22,d], J. Mitrevski[70], R.K. Mommsen[44], N.K. Mondal[29], R.W. Moore[6], T. Moulik[58], G.S. Muanza[15], M. Mulhearn[70], O. Mundal[22], L. Mundim[3], E. Nagy[15], M. Naimuddin[50], M. Narain[77], H.A. Neal[64], J.P. Negret[8], P. Neustroev[40], H. Nilsen[23], H. Nogima[3], S.F. Novaes[5], T. Nunnemann[25], D.C. O'Neil[6], G. Obrant[40], C. Ochando[16], D. Onoprienko[59], N. Oshima[50], N. Osman[43], J. Osta[55], R. Otec[10], G.J. Otero y Garzón[50], M. Owen[44], P. Padley[80], M. Pangilinan[77], N. Parashar[56], S.-J. Park[22,d], S.K. Park[31], J. Parsons[70], R. Partridge[77], N. Parua[54], A. Patwa[73], G. Pawloski[80], B. Penning[23], M. Perfilov[38], K. Peters[44], Y. Peters[26], P. Pétroff[16], M. Petteni[43], R. Piegaia[1], J. Piper[65], M.-A. Pleier[22], P.L.M. Podesta-Lerma[33,f], V.M. Podstavkov[50], Y. Pogorelov[55], M.-E. Pol[2], P. Polozov[37], B.G. Pope[65], A.V. Popov[39], C. Potter[6], W.L. Prado da Silva[3],

H.B. Prosper[49], S. Protopopescu[73], J. Qian[64], A. Quadt[22,d], B. Quinn[66], A. Rakitine[42], M.S. Rangel[2], K. Ranjan[28], P.N. Ratoff[42], P. Renkel[79], P. Rich[44], M. Rijssenbeek[72], I. Ripp-Baudot[19], F. Rizatdinova[76], S. Robinson[43], R.F. Rodrigues[3], M. Rominsky[75], C. Royon[18], P. Rubinov[50], R. Ruchti[55], G. Safronov[37], G. Sajot[14], A. Sánchez-Hernández[33], M.P. Sanders[17], B. Sanghi[50], G. Savage[50], L. Sawyer[60], T. Scanlon[43], D. Schaile[25], R.D. Schamberger[72], Y. Scheglov[40], H. Schellman[53], T. Schliephake[26], S. Schlobohm[82], C. Schwanenberger[44], A. Schwartzman[68], R. Schwienhorst[65], J. Sekaric[49], H. Severini[75], E. Shabalina[51], M. Shamim[59], V. Shary[18], A.A. Shchukin[39], R.K. Shivpuri[28], V. Siccardi[19], V. Simak[10], V. Sirotenko[50], P. Skubic[75], P. Slattery[71], D. Smirnov[55], G.R. Snow[67], J. Snow[74], S. Snyder[73], S. Söldner-Rembold[44], L. Sonnenschein[17], A. Sopczak[42], M. Sosebee[78], K. Soustruznik[9], B. Spurlock[78], J. Stark[14], V. Stolin[37], D.A. Stoyanova[39], J. Strandberg[64], S. Strandberg[41], M.A. Strang[69], E. Strauss[72], M. Strauss[75], R. Ströhmer[25], D. Strom[53], L. Stutte[50], S. Sumowidagdo[49], P. Svoisky[35], A. Sznajder[3], A. Tanasijczuk[1], W. Taylor[6], B. Tiller[25], F. Tissandier[13], M. Titov[18], V.V. Tokmenin[36], I. Torchiani[23], D. Tsybychev[72], B. Tuchming[18], C. Tully[68], P.M. Tuts[70], R. Unalan[65], L. Uvarov[40], S. Uvarov[40], S. Uzunyan[52], B. Vachon[6], P.J. van den Berg[34], R. Van Kooten[54], W.M. van Leeuwen[34], N. Varelas[51], E.W. Varnes[45], I.A. Vasilyev[39], P. Verdier[20], L.S. Vertogradov[36], M. Verzocchi[50], D. Vilanova[18], F. Villeneuve-Seguier[43], P. Vint[43], P. Vokac[10], M. Voutilainen[67,g], R. Wagner[68], H.D. Wahl[49], M.H.L.S. Wang[50], J. Warchol[55], G. Watts[82], M. Wayne[55], G. Weber[24], M. Weber[50,h], L. Welty-Rieger[54], A. Wenger[23,i], N. Wermes[22], M. Wetstein[61], A. White[78], D. Wicke[26], M.R.J. Williams[42], G.W. Wilson[58], S.J. Wimpenny[48], M. Wobisch[60], D.R. Wood[63], T.R. Wyatt[44], Y. Xie[77], C. Xu[64], S. Yacoob[53], R. Yamada[50], W.-C. Yang[44], T. Yasuda[50], Y.A. Yatsunenko[36], H. Yin[7], K. Yip[73], H.D. Yoo[77], S.W. Youn[53], J. Yu[78], C. Zeitnitz[26], S. Zelitch[81], T. Zhao[82], B. Zhou[64], J. Zhu[72], M. Zielinski[71], D. Zieminska[54], A. Zieminski[54,‡], L. Zivkovic[70], V. Zutshi[52], and E.G. Zverev[38]

(The DØ Collaboration)

[1] *Universidad de Buenos Aires, Buenos Aires, Argentina*
[2] *LAFEX, Centro Brasileiro de Pesquisas Físicas, Rio de Janeiro, Brazil*
[3] *Universidade do Estado do Rio de Janeiro, Rio de Janeiro, Brazil*
[4] *Universidade Federal do ABC, Santo André, Brazil*
[5] *Instituto de Física Teórica, Universidade Estadual Paulista, São Paulo, Brazil*
[6] *University of Alberta, Edmonton, Alberta, Canada, Simon Fraser University, Burnaby, British Columbia, Canada, York University, Toronto, Ontario, Canada, and McGill University, Montreal, Quebec, Canada*
[7] *University of Science and Technology of China, Hefei, People's Republic of China*
[8] *Universidad de los Andes, Bogotá, Colombia*
[9] *Center for Particle Physics, Charles University, Prague, Czech Republic*
[10] *Czech Technical University, Prague, Czech Republic*
[11] *Center for Particle Physics, Institute of Physics, Academy of Sciences of the Czech Republic, Prague, Czech Republic*
[12] *Universidad San Francisco de Quito, Quito, Ecuador*
[13] *LPC, Université Blaise Pascal, CNRS/IN2P3, Clermont, France*
[14] *LPSC, Université Joseph Fourier Grenoble 1, CNRS/IN2P3, Institut National Polytechnique de Grenoble, Grenoble, France*
[15] *CPPM, Aix-Marseille Université, CNRS/IN2P3, Marseille, France*
[16] *LAL, Université Paris-Sud, IN2P3/CNRS, Orsay, France*
[17] *LPNHE, IN2P3/CNRS, Universités Paris VI and VII, Paris, France*
[18] *CEA, Irfu, SPP, Saclay, France*
[19] *IPHC, Université Louis Pasteur, CNRS/IN2P3, Strasbourg, France*
[20] *IPNL, Université Lyon 1, CNRS/IN2P3, Villeurbanne, France and Université de Lyon, Lyon, France*
[21] *III. Physikalisches Institut A, RWTH Aachen University, Aachen, Germany*
[22] *Physikalisches Institut, Universität Bonn, Bonn, Germany*
[23] *Physikalisches Institut, Universität Freiburg, Freiburg, Germany*
[24] *Institut für Physik, Universität Mainz, Mainz, Germany*
[25] *Ludwig-Maximilians-Universität München, München, Germany*
[26] *Fachbereich Physik, University of Wuppertal, Wuppertal, Germany*
[27] *Panjab University, Chandigarh, India*
[28] *Delhi University, Delhi, India*
[29] *Tata Institute of Fundamental Research, Mumbai, India*
[30] *University College Dublin, Dublin, Ireland*
[31] *Korea Detector Laboratory, Korea University, Seoul, Korea*
[32] *SungKyunKwan University, Suwon, Korea*

[33] CINVESTAV, Mexico City, Mexico
[34] FOM-Institute NIKHEF and University of Amsterdam/NIKHEF, Amsterdam, The Netherlands
[35] Radboud University Nijmegen/NIKHEF, Nijmegen, The Netherlands
[36] Joint Institute for Nuclear Research, Dubna, Russia
[37] Institute for Theoretical and Experimental Physics, Moscow, Russia
[38] Moscow State University, Moscow, Russia
[39] Institute for High Energy Physics, Protvino, Russia
[40] Petersburg Nuclear Physics Institute, St. Petersburg, Russia
[41] Lund University, Lund, Sweden, Royal Institute of Technology and Stockholm University, Stockholm, Sweden, and Uppsala University, Uppsala, Sweden
[42] Lancaster University, Lancaster, United Kingdom
[43] Imperial College, London, United Kingdom
[44] University of Manchester, Manchester, United Kingdom
[45] University of Arizona, Tucson, Arizona 85721, USA
[46] Lawrence Berkeley National Laboratory and University of California, Berkeley, California 94720, USA
[47] California State University, Fresno, California 93740, USA
[48] University of California, Riverside, California 92521, USA
[49] Florida State University, Tallahassee, Florida 32306, USA
[50] Fermi National Accelerator Laboratory, Batavia, Illinois 60510, USA
[51] University of Illinois at Chicago, Chicago, Illinois 60607, USA
[52] Northern Illinois University, DeKalb, Illinois 60115, USA
[53] Northwestern University, Evanston, Illinois 60208, USA
[54] Indiana University, Bloomington, Indiana 47405, USA
[55] University of Notre Dame, Notre Dame, Indiana 46556, USA
[56] Purdue University Calumet, Hammond, Indiana 46323, USA
[57] Iowa State University, Ames, Iowa 50011, USA
[58] University of Kansas, Lawrence, Kansas 66045, USA
[59] Kansas State University, Manhattan, Kansas 66506, USA
[60] Louisiana Tech University, Ruston, Louisiana 71272, USA
[61] University of Maryland, College Park, Maryland 20742, USA
[62] Boston University, Boston, Massachusetts 02215, USA
[63] Northeastern University, Boston, Massachusetts 02115, USA
[64] University of Michigan, Ann Arbor, Michigan 48109, USA
[65] Michigan State University, East Lansing, Michigan 48824, USA
[66] University of Mississippi, University, Mississippi 38677, USA
[67] University of Nebraska, Lincoln, Nebraska 68588, USA
[68] Princeton University, Princeton, New Jersey 08544, USA
[69] State University of New York, Buffalo, New York 14260, USA
[70] Columbia University, New York, New York 10027, USA
[71] University of Rochester, Rochester, New York 14627, USA
[72] State University of New York, Stony Brook, New York 11794, USA
[73] Brookhaven National Laboratory, Upton, New York 11973, USA
[74] Langston University, Langston, Oklahoma 73050, USA
[75] University of Oklahoma, Norman, Oklahoma 73019, USA
[76] Oklahoma State University, Stillwater, Oklahoma 74078, USA
[77] Brown University, Providence, Rhode Island 02912, USA
[78] University of Texas, Arlington, Texas 76019, USA
[79] Southern Methodist University, Dallas, Texas 75275, USA
[80] Rice University, Houston, Texas 77005, USA
[81] University of Virginia, Charlottesville, Virginia 22901, USA and
[82] University of Washington, Seattle, Washington 98195, USA

(Dated: October 31, 2008)

The first search in $p\bar{p}$ collisions at $\sqrt{s} = 1.96$ TeV for the production of neutral Higgs bosons in association with bottom quarks and decaying in two tau leptons is presented. The cross section for this process is enhanced in many extensions of the standard model (SM), such as its minimal supersymmetric extension (MSSM) at large $\tan\beta$. The data, corresponding to an integrated luminosity of 328 pb^{-1}, were collected with the D0 detector at the Fermilab Tevatron Collider. An upper limit is set on the production cross section of neutral Higgs bosons in the mass range of 90 to 150 GeV, and this limit is used to exclude part of the MSSM parameter space.

PACS numbers: 14.80.Cp, 12.60.Fr, 12.60.Jv, 13.85.Rm

In the minimal supersymmetric extension of the standard model (MSSM), the Higgs sector consists of five

physical Higgs bosons: two neutral scalars, h and H (with $m_h < m_H$ by convention), one neutral pseudoscalar, A, and a charged pair, $H^{\pm}$. At leading order (LO), the coupling of the neutral Higgs bosons to down-type quarks is proportional to $\tan\beta$, where $\tan\beta$ is the ratio of the vacuum expectation values of the two Higgs doublets. The production cross section of a neutral Higgs boson in association with a down-type quark, such as the b quark, is therefore proportional to $\tan^2\beta$ (at LO). Thus, the $b\phi$ ($\phi = h, H, A$) production mechanism provides a natural mode to search for a neutral Higgs boson at high $\tan\beta$ in the MSSM [1].

In most of the MSSM parameter phase space, the neutral scalar Higgs bosons h and H decay $\sim$90% of the time into a pair of b quarks, and $\sim$10% of the time into a pair of tau leptons. The neutral pseudoscalar A decays into $b\bar{b}$ or $\tau^+\tau^-$ in all of the parameter space, with similar branching ratios ($\sim$90% and $\sim$10%, respectively). In this Letter, we present a search for the production of a neutral Higgs boson in association with a b quark, with the subsequent decay of the Higgs boson into two tau leptons, using data collected by the D0 experiment in $p\bar{p}$ collisions at $\sqrt{s} = 1.96$ TeV at the Fermilab Tevatron collider. We perform the analysis using the final state where one tau decays leptonically into a muon ($\tau \to \mu\nu_\mu\nu_\tau$), and the other tau decays hadronically into a narrow jet ($\tau \to \tau_h\nu_\tau$, where τ_h denotes the hadronic tau jet).

The $b\phi \to b\tau^+\tau^-$ search channel is complementary to the $b\phi \to bb\bar{b}$ [2] and the inclusive $\phi \to \tau^+\tau^-$ [3] searches. The $\tau^+\tau^-$ decay mode of the Higgs boson is less sensitive than the $b\bar{b}$ decay to the large supersymmetric radiative corrections on the production cross section and decay width [1]. Experimentally, the $b\tau^+\tau^-$ channel presents a clean signature which does not suffer from the large heavy-flavor multi-jet background of the $bb\bar{b}$ channel, and is less affected by the $Z \to \tau^+\tau^-$ background than the inclusive $\phi \to \tau^+\tau^-$ channel.

The D0 detector [4] consists of a central tracking system, comprising a silicon microstrip tracker and a central fiber tracker, both within a 2 T solenoidal magnet; a liquid-argon and uranium calorimeter, divided into a central calorimeter and two end calorimeters; and a muon system, consisting of three layers of tracking detectors and scintillation trigger counters.

This analysis considers data collected by the D0 experiment between August 2002 and June 2004. Two single-muon triggers are used, requiring a muon with transverse momentum (p_T) greater than either 3 or 5 GeV and a track with $p_T > 10$ GeV. The total integrated luminosity for the selected triggers is 328 ± 20 pb^{-1} [5].

Signal events are simulated using the process $p\bar{p} \to b\phi \to b\tau^+\tau^-$ in PYTHIA [6], where one of the tau leptons is forced to decay leptonically into a muon and the second tau is free to decay to all allowed modes; the b quark is generated with $p_T > 15$ GeV and $|\eta| < 2.5$, where $\eta = -\ln[\tan(\theta/2)]$ is the pseudorapidity and θ is the polar angle relative to the proton beam direction. Background processes such as $t\bar{t}$, W+jets and WW production are simulated using ALPGEN [7] interfaced with PYTHIA for showering and fragmentation. Additional $p\bar{p}$ interactions are modeled with PYTHIA according to a Poisson distribution with mean of 0.4 events, which corresponds to the expected average multiplicity in the data. The simulated events are processed through a GEANT-based [8] simulation of the D0 detector and reconstructed with the same software as the collider data. They are also weighted on an event-by-event basis by the trigger efficiency parametrization measured in the data. The trigger efficiency, estimated on the simulated signal sample after selecting $\mu\tau_h$ pairs, is (62 ± 1)%.

There are three types of physics objects used in this analysis: muons, hadronic taus, and jets. All selected objects are required to be associated with the same primary vertex within 1 cm along the beam direction.

Muons are reconstructed from patterns of hits in the muon detectors matched to isolated central tracks, and are required to have $p_T > 12$ GeV.

Hadronically decaying taus are characterized by a narrow isolated jet with low track multiplicity. We distinguish three tau types: (1) a single track with energy deposited in the hadronic calorimeter, (2) a single track with energy deposited both in the hadronic and electromagnetic calorimeters, and (3) three tracks with corresponding energy deposited in the calorimeter.

After an initial selection of tau candidates based on the transverse energy (E_T) of the calorimeter cluster, sum of the track transverse momenta, and isolation and width of the associated calorimeter energy deposits, the candidates are further discriminated against jets using a neural network (NN) which has been trained separately for each tau type [9]. For types 1 and 2, tau candidates are required to have a NN output greater than 0.8. For type 3 tau candidates, because of the larger multijet background, the NN selection is tightened to 0.98. The average tau identification efficiency in signal events is $\sim$62%.

Jets are reconstructed from clusters of energy in the calorimeter using the D0 Run II midpoint cone algorithm with a radius of 0.5 [10]. Jet energies are corrected to the particle level. Events are required to have at least one jet identified as originating from a b quark (b tagged) and with $p_T > 15$ GeV and $|\eta| < 2.5$. Jets are b tagged using an algorithm that computes the probability that the jet originated from a b hadron, based on the impact parameter of the tracks associated with the jet [11]. For a jet of $p_T = 20$ GeV and $|\eta| < 2.5$, as is typical for signal events, the b-tagging efficiency measured in data is $\sim$40%, whereas the probability to tag a light-flavor jet is $\sim$1%. A parameterization of the b-tagging efficiency measured in data is applied to each simulated jet, according to its p_T, η and flavor.

Main backgrounds to the $b\phi \to b\tau^+\tau^- \to b\mu\tau_h$ process are multijet, Z+jets and $t\bar{t}$ production. Smaller back-

ground contributions originate from W+jets and WW production. The multijet and Z+jets backgrounds are estimated from the data, whereas all other backgrounds are estimated from the Monte Carlo (MC) simulation.

A multijet background event typically consists of two or more jets, with one jet misidentified as a hadronic tau, a real or misidentified b jet, and a muon from a heavy-flavor decay that appears isolated. Since the charge of the muon is not correlated with the charge of the hadronic tau candidate, the multijet background tends to have equal amounts of opposite-sign (OS) and same-sign (SS) $\mu\tau_h$ pairs. In contrast, the signal should contain only opposite-sign $\mu\tau_h$ pairs coming from the Higgs decay. Thus, we require that the reconstructed muon and hadronic tau have opposite charges. The multijet background in the OS sample is estimated from the SS events in the data as follows: first, the SS yield is corrected for non-multijet backgrounds by subtracting these based on MC estimates; second, the corrected SS multijet yield is multiplied by the probability of a jet to be misidentified as a hadronic tau; third, a correction is applied to account for a small asymmetry observed in OS and SS multijet control samples; finally, the probability of a multijet event to have at least one b-tagged jet is applied.

The production of a Z boson in association with jets contributes as a background via $Z \to \tau^+\tau^- \to \mu\tau_h$ and $Z \to \mu^+\mu^-$ decays, and where one of the jets is a real or misidentified b jet. In the case of $Z \to \mu^+\mu^-$, one of the muons is misidentified as a hadronic tau. The contribution from both real and misidentified b jet backgrounds, in either Z decay channel, is estimated by measuring the fraction of b-tagged events in $Z \to \mu^+\mu^-$ data, found to be $(2.5\pm0.4)\%$, and multiplying it by the estimated number of $Z(\to \mu\tau_h)$+jets events in data before b tagging.

After b tagging, $t\bar{t}$ production is the dominant background. Such events are characterized by having higher p_T objects than those in signal events. Therefore, in order to reduce the $t\bar{t}$ background, we use a neural network (KNN) which exploits kinematic differences between signal and background, based on four variables: the sum of the transverse momenta of all jets in the event (excluding the tau jet), the missing transverse energy $\not\!\!E_T$ (constructed from calorimeter cells and the momenta of muons, and corrected for the energy response of taus and jets), the jet multiplicity, and the azimuthal angular separation between the muon and the tau jet. The neural network training is performed using a background MC sample of $t\bar{t}$ events where both W bosons decay leptonically ($t\bar{t} \to \mu\tau_h$) and a signal MC sample consisting of $b\phi \to b\tau^+\tau^- \to b\mu\tau_h$ events with a mixture of different Higgs masses. In both samples, the events used passed all selection criteria except b tagging. The KNN selection is optimized separately for each tau type. Events with type 1 and 3 taus have low $t\bar{t}$ background and do not benefit from a KNN selection. Requiring a KNN output greater than 0.4 has a signal efficiency of $\sim$95% and is found to be optimal for events with type 2 taus. The amount of $t\bar{t}$ background remaining after the KNN selection is estimated from MC.

Systematic uncertainties affecting both signal and background predictions based on MC are: integrated luminosity (signal: 6%, background: <1%) [5]; trigger efficiency (1.1%); tau identification (signal: 3-9%, background: <0.4%); tau energy scale (10%); jet identification (signal: 6-9%, background: <7%); jet energy scale (signal: 7-10%, background: <4%); b-jet identification (signal: 5%, background: <2%); and uncertainties on the signal (10%) and $t\bar{t}$, W+jets (20-30%) and WW theoretical cross sections. For backgrounds derived from data, the systematic uncertainties result from the limited statistics of the control data samples.

The estimated number of events from the various backgrounds and the observed number of events in the data for the three tau types are presented in Table I. Also shown are the signal acceptance and the number of expected signal events for a Higgs mass $M_\phi = 120$ GeV and $\tan\beta = 80$. The visible mass $M_{\rm vis}$ distributions, constructed from the four-vector momenta of the muon, hadronic tau, and missing momentum [3], for the data and SM prediction are shown in Fig. 1. No visible excess over the SM prediction is observed in the data.

TABLE I: Expected number of events for backgrounds, number of observed events in data, signal acceptance for events with at least one muon and expected number of signal events for $M_\phi = 120$ GeV and $\tan\beta = 80$, for each hadronic tau type. Quoted uncertainties represent statistical and systematic added in quadrature.

	Type 1	Type 2	Type 3
Multijet	0.60 ± 0.22	0.48 ± 0.14	0.95 ± 0.16
Z+jets	0.34 ± 0.09	1.50 ± 0.27	0.25 ± 0.08
$t\bar{t}$	0.28 ± 0.06	0.65 ± 0.18	0.21 ± 0.05
W+jets	0.009 ± 0.005	0.073 ± 0.036	0.28 ± 0.12
WW	0	0.014 ± 0.004	0
Total Background	1.22 ± 0.19	2.71 ± 0.33	1.68 ± 0.15
Observed	0	1	2
Signal Accept. (%)	0.15 ± 0.03	0.87 ± 0.14	0.27 ± 0.05
Expected Signal	0.68 ± 0.15	3.9 ± 0.7	1.2 ± 0.2

Upper limits on the production cross section times branching ratio are set using a modified frequentist approach [12]. In order to maximize the sensitivity, each tau type is treated as a separate channel and the kinematic differences between signal and background are exploited by using the $M_{\rm vis}$ distribution in the limit calculation. In each channel, the $M_{\rm vis}$ distribution is split into three bins: 30-60, 60-85 and 85-180 GeV (see Fig. 1). The choice of bin size is driven by the available statistics in data to estimate the multijet background. Figure 2 shows the 95% confidence level (C.L.) upper limits on the production cross section times branching ratio as a function of the Higgs mass. Despite the $\sim$1:9 branching ratio of the

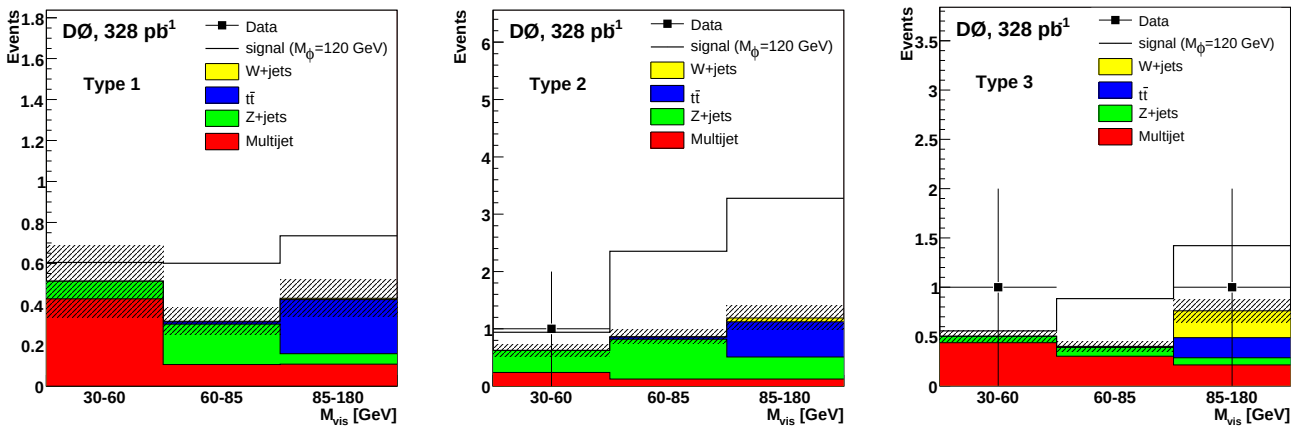

FIG. 1: Visible mass distributions for each tau type. Histograms show the signal and various backgrounds, points show the data. The error bands indicate the total uncertainty on the background estimation.

$\tau^+\tau^-$ to $b\bar{b}$ Higgs decay modes, the upper limit on the $b\phi$ production cross section obtained by this analysis is competitive with the corresponding one in the $b\phi \to bb\bar{b}$ channel [2], particularly at low M_ϕ.

Using the cross section limit for $b\phi$ production, we can exclude regions of $(m_A, \tan\beta)$ parameter space in the MSSM. Beyond LO, the masses and couplings of the Higgs bosons in the MSSM depend (through radiative corrections) on additional SUSY parameters, besides m_A and $\tan\beta$. Thus, we derive limits on $\tan\beta$ as a function of m_A in two specific, commonly used scenarios (assuming a CP-conserving Higgs sector): the m_h^{max} scenario and the no-mixing scenario [1]. The production cross sections, widths and branching ratios for the Higgs bosons are calculated over the mass range 90-150 GeV using the MCFM and FEYNHIGGS programs [13, 14]. Since at large $\tan\beta$ the A boson is nearly degenerate in mass with either the h or the H boson, their production cross sections are added. As shown in Fig. 2, this analysis excludes a large portion of the MSSM parameter space. For negative values of the Higgsino mass parameter μ, the $\tau^+\tau^-$ decay mode explored here has comparable sensitivity to the $b\bar{b}$ decay mode [2]. For positive values of μ, however, the $\tau^+\tau^-$ mode is superior to the $b\bar{b}$ mode, as it does not suffer from the effect of the large supersymmetric radiative corrections to the Higgs production cross section and decay width [1]. Compared to the inclusive $\phi \to \tau^+\tau^-$ channel [3], for the same integrated luminosity the $b\phi \to b\tau^+\tau^-$ channel offers increased sensitivity in the low M_ϕ region, as it does not suffer from the large $Z \to \tau^+\tau^-$ background.

In summary, we have presented results from a search for $b\phi \to b\tau^+\tau^-$ production, resulting in significant portions of the MSSM parameter space being excluded in two specific scenarios. This analysis is found to be both competitive and complementary to other searches in the $b\phi \to bb\bar{b}$ and inclusive $\phi \to \tau^+\tau^-$ channels, hence contributing to the overall sensitivity at the Tevatron.

We thank the staffs at Fermilab and collaborating institutions, and acknowledge support from the DOE and NSF (USA); CEA and CNRS/IN2P3 (France); FASI, Rosatom and RFBR (Russia); CNPq, FAPERJ, FAPESP and FUNDUNESP (Brazil); DAE and DST (India); Colciencias (Colombia); CONACyT (Mexico); KRF and KOSEF (Korea); CONICET and UBACyT (Argentina); FOM (The Netherlands); STFC (United Kingdom); MSMT and GACR (Czech Republic); CRC Program, CFI, NSERC and WestGrid Project (Canada); BMBF and DFG (Germany); SFI (Ireland); The Swedish Research Council (Sweden); CAS and CNSF (China); and the Alexander von Humboldt Foundation (Germany).

[a] Visitor from Augustana College, Sioux Falls, SD, USA.
[b] Visitor from Rutgers University, Piscataway, NJ, USA.
[c] Visitor from The University of Liverpool, Liverpool, UK.
[d] Visitor from II. Physikalisches Institut, Georg-August-University, Göttingen, Germany.
[e] Visitor from Centro de Investigacion en Computacion - IPN, Mexico City, Mexico.
[f] Visitor from ECFM, Universidad Autonoma de Sinaloa, Culiacán, Mexico.
[g] Visitor from Helsinki Institute of Physics, Helsinki, Finland.
[h] Visitor from Universität Bern, Bern, Switzerland.
[i] Visitor from Universität Zürich, Zürich, Switzerland.
[‡] Deceased.

[1] M. Carena, S. Heinemeyer, C.E.M. Wagner and G. Weiglein, Eur. Phys. J. C **45**, 797 (2006).

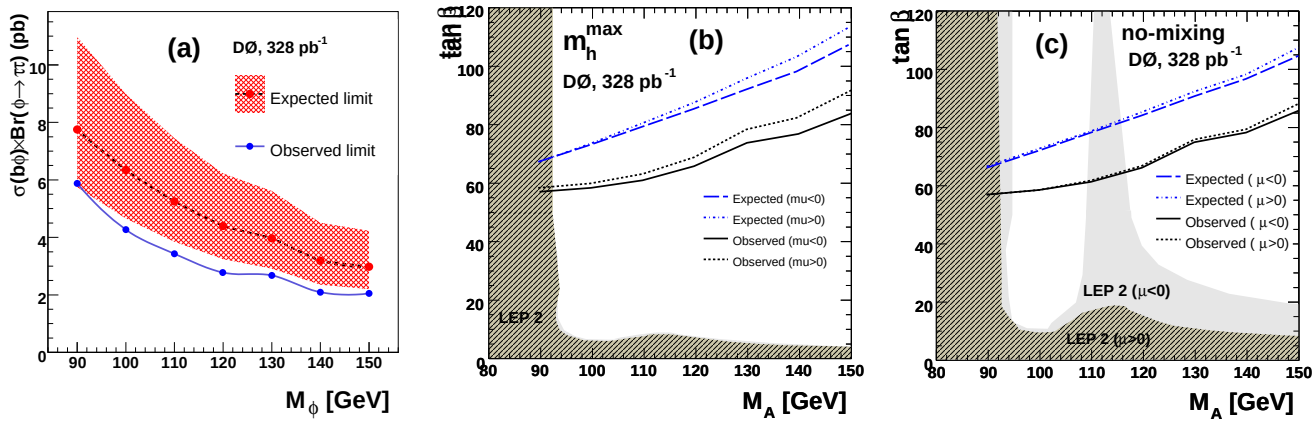

FIG. 2: (a) The 95% C.L. expected and observed limits on the cross section times branching ratio for $p\bar{p} \to b\phi \to b\tau^+\tau^-$ production as a function of the Higgs mass. Also shown is the ± 1 standard deviation band on the expected limit. These cross section limits are used to derive exclusion regions in the $(m_A, \tan\beta)$ plane for (b) the m_h^{max} and (c) the no-mixing scenarios of the MSSM, for both $\mu = +200$ GeV and $\mu = -200$ GeV. Also shown is the region excluded by the LEP experiments.

[2] D0 Collaboration, V.M. Abazov *et al.*, arXiv:0805.3556 [hep-ex] (2008), accepted by Phys. Rev. Lett.

[3] CDF Collaboration, A. Abulencia *et al.*, Phys. Rev. Lett. **96**, 011802 (2006); D0 Collaboration, V.M. Abazov *et al.*, Phys. Rev. Lett. **101**, 071804 (2008).

[4] D0 Collaboration, V.M. Abazov *et al.*, Nucl. Instrum. Methods Phys. Res. A **565**, 463 (2006).

[5] T. Andeen *et al.*, FERMILAB-TM-2365 (2007).

[6] T. Sjöstrand *et al.*, Comput. Phys. Commun. **135**, 238 (2001).

[7] M. Mangano *et al.*, JHEP **0307**, 1 (2003).

[8] R. Brun and F. Carminati, CERN Program Library Long Writeup W5013, 1993 (unpublished).

[9] D0 Collaboration, V.M. Abazov *et al.*, Phys. Rev. D **71**, 072004 (2005) [Erratum-ibid. **77**, 039901(2008)]

[10] G.C. Blazey *et al.*, arXiv:hep-ex/0005012 (2000).

[11] S. Greder, FERMILAB-THESIS-2004-28.

[12] T. Junk, Nucl. Instrum. Methods Phys. Res. A **434**, 435 (1999).

[13] J. Campbell, R.K. Ellis, F. Maltoni and S. Willenbrock, Phys. Rev. D **67**, 095002 (2003).

[14] S. Heinemeyer, W. Hollik and G. Weiglein, Comput. Phys. Commun. **124**, 76 (2000).